

# Pulsating solitons, chaotic solitons, period doubling, and pulse coexistence in mode-locked lasers: Complex Ginzburg-Landau equation approach

N. Akhmediev,<sup>1</sup> J. M. Soto-Crespo,<sup>2</sup> and G. Town<sup>3</sup>

<sup>1</sup>*Optical Sciences Centre, Research School of Physical Sciences and Engineering, Institute of Advanced Studies, Australian National University, Australian Capital Territory 0200, Australia*

<sup>2</sup>*Instituto de Óptica, Consejo Superior de Investigaciones Científicas, Serrano 121, 28006 Madrid, Spain*

<sup>3</sup>*School of Electrical and Information Engineering (J03), University of Sydney, NSW 2006, Australia*

(Received 11 August 2000; published 9 April 2001)

The complex Ginzburg-Landau equation (CGLE) is a standard model for pulse generation in mode-locked lasers with fast saturable absorbers. We have found complicated pulsating behavior of solitons of the CGLE and regions of their existence in the five-dimensional parameter space. We have found zero-velocity, moving and exploding pulsating localized structures, period doubling (PD) of pulsations and the sequence of PD bifurcations. We have also found chaotic pulsating solitons. We have plotted regions of parameters of the CGLE where pulsating solutions exist. We also demonstrate the coexistence (bi- and multistability) of different types of pulsating solutions in certain regions of the parameter space of the CGLE.

DOI: 10.1103/PhysRevE.63.056602

PACS number(s): 42.65.-k, 47.20.Ky

## I. INTRODUCTION

Passive mode locking allows the generation of self-shaped ultrashort pulses in a laser system. It was realized in a number of works that the pulses generated by mode-locked fiber lasers were solitons [1–4]. Apart from this very important application, the mode-locked laser is a nonlinear system, which can have a very rich dynamics that includes not only the generation of a periodic train of well-shaped pulses but also much more complicated behaviors. In fact, the generation of stable pulses is possible in a very narrow range of the laser parameters and requires their careful adjustment. More generally, the pulses change their shape from one round trip to another and have complicated dynamics in time. They might have periodic behavior in a time scale larger than the round-trip time. As a particular result, the laser might have period-doubling, tripling, etc. behavior as well as oscillations of the pulse shape with periods that are not necessarily commensurate with the round trip time. If there are several periods involved in this dynamics, then the pulse-shape evolution in time might seem chaotic. This general dynamics and the particular effect of trapping into the regime of stable pulse generation is the phenomenon that deserves a detailed theoretical and numerical investigation from various points of view.

Period doubling bifurcations and chaotic behavior of nonlinear systems have been long discussed subjects in the literature. In optics, period-doubling bifurcations have been found experimentally in various laser systems. These include semiconductor lasers [5], femtosecond solid-state lasers [6], *F*-center lasers [7,8], fiber lasers [9,10], nonlinear cavities [11,12], and gaseous lasers [13]. Period doubling in time of a train of pulses has been observed in mode-locked lasers [6,7] and nonlinear fiber ring resonators [10]. Originally, period-doubling phenomenon was numerically found for the simple case of a logistic map [14]. However, period doubling has not been particularly related to solitons.

In previous works, period-doubling bifurcations in lasers

have been described using various approaches including recursion relations [7], infinite-dimensional map with nonlinear Schrödinger equation (NLSE) [10], rate equations [15], logistic map [16], equations for nonlinear polarization mixing [17], free-electron laser equations [18], and other methods. Period-doubling bifurcations have been attributed to the presence of ion pairs in the highly doped erbium fiber [19]. Later, it was realized that the presence of saturable absorbers in general form can be responsible for this behavior. Dispersion has also been found to be important in the period-doubling phenomenon [10]. Although it was well known that the mode-locked laser operation can be described, in some approximations, using the complex Ginzburg-Landau equation (CGLE) [20–23], period doubling and route to chaos have not been studied yet theoretically using this approach.

In the present paper we study pulsating soliton solutions of the CGLE, which by themselves constitute a surprising phenomenon. We recall that Hamiltonian systems do not have pulsating soliton solutions. Even if excited initially, pulsating solitons are subjected to restructuring and evolve to stationary solitons [24]. An exception from this rule are the integrable models where pulsating structures are nonlinear superpositions of fundamental solitons [25]. Dissipative systems, in contrast to Hamiltonian ones, admit pulsating solitons. Interestingly enough, they do not appear from the integrable limit and hence do not have anything in common with the nonlinear superposition of fundamental solitons of the NLSE [25]. The parameters of the CGLE have to be far enough from the NLSE limit in order to obtain pulsating solitons. One example of a pulsating soliton of the cubic-quintic CGLE has been presented previously by Deissler and Brand [26]. This is the only example we are aware of and it has been found in the normal dispersion regime, where solitons do not exist in the integrable limit. In fact, as we shall show below, this is not the only case where pulsating solutions exist. They do exist in the anomalous dispersion region and, moreover, the variety of these solutions and their region of existence is huge. In either case, pulsating solutions can-

not be found by extrapolating from those in the integrable limit.

The study of pulsating solutions would not be complete without the cases when the periodicity of pulsations becomes not perfect. The pulse behavior in time can be more complicated and even chaotic at certain values of the parameters. The system can enter into a chaotic regime in various ways including the classical one through period-doubling bifurcations. In our opinion, the most interesting phenomenon is that stationary stable solitons can coexist with the chaotic regime of soliton propagation. Which solution is excited depends to a great extent on the initial conditions. Clearly, chaotic and regular solutions are well separated in the functional space so that they do not transform to each other unless we disturb the solution with a finite perturbation or change the parameters of the system to the extent that one of the solutions becomes unstable. It is not surprising that two stable solutions can coexist. However, the coexistence of chaotic and regular solution rarely happens.

In addition to presenting new classes of pulsating solitons, we describe the period-doubling phenomenon using the CGLE. This description fills the gap in theory that existed before and shows that the phenomenon falls into the general class of chaotic behavior and routes to chaos. Moreover, we show that new pulsating solitons can coexist both with chaotic solutions and with stationary pulses leading to the phenomenon of bistability. This complex bistability of chaotic solutions with regular ones might cause a peculiar behavior of ultrashort pulse lasers.

It was a long standing controversial question how a laser system enters into chaotic regime. The transition may happen abruptly and not necessarily through the sequence of period-doubling bifurcations [10]. In fact, various scenarios of the route to chaos have been observed. Our approach gives the answer to this question too. We study regions of chaotic behavior in the five-dimensional parameter space of the CGLE whose borders form a four-dimensional surface of complicated shape. The transition to chaos from the region of regular behavior depends very much on where this surface is crossed. Our simulations show explicitly that the route to chaos can be either through the sequence of period-doubling bifurcations or we can have an abrupt transition. Moreover, our study shows that the borders are not necessarily sharp and around them some regions of bistability can exist.

Our continuous model takes into account the major physical effects occurring in a laser cavity such as dispersion, self-phase modulation, spectral filtering, and gain/loss (both linear and nonlinear). A delicate balance between them gives rise to the majority of the effects observed experimentally. We observe even period-3, period-5, and period-6 solutions in our model. Note that period 6 pulse generation has been observed recently in a nonlinear fiber ring resonator by Coen *et al.* [10].

We should keep in mind that in principle there will be differences between the results in our model and in real systems because of the finite round-trip time which every laser system has. In the case of the CGLE model the period of pulsations can vary continuously rather than in discrete steps. Moreover, complicated phenomena related to the interplay

between the periodicity in the system and pulsations in time might arise. However, in this paper we are interested in the occurrence of pulsations in a continuous model and their evolution for a given set of CGLE parameters. The effect of discreteness can be taken into account in specific applications. At present, our main aim is to investigate the results predicted by the powerful CGLE continuous model rather than to look for the origin of possible complications.

The rest of the paper is organized as follows. In Sec. II we present the Master equation which we are solving. Section III presents the numerical scheme used in the simulations. Section IV shows a variety of examples of pulsating solitons of the CGLE, including some highly unusual pulsations like exploding and creeping solitons. The sequence of period doubling bifurcations of the pulsating solitons and other routes to chaotic pulsations is discussed in Sec. V. The possibility of coexistence of various solitons including pulsating and chaotic ones is described in Sec. VI. The regions of existence of various pulsating and chaotic solutions in the parameter space of the CGLE are given in Sec. VII. The results are discussed in Sec. VIII and finally Sec. IX summarizes our main conclusions.

## II. CGLE EQUATION

The quintic complex Ginzburg-Landau equation has been used to describe a variety of physical phenomena. In optics it is often used to model several types of passively mode-locked lasers with fast saturable absorbers [20–23], parametric oscillators [27], and transverse soliton effects in wide aperture lasers [28–33]. In spite of the fact that lumped effects are present in any laser, in many cases its operation is well described as a distributed system. In this context the quintic CGLE has the following form [34]:

$$i\psi_z + \frac{D}{2}\psi_{tt} + |\psi|^2\psi + \nu|\psi|^4\psi = i\delta\psi + i\epsilon|\psi|^2\psi + i\beta\psi_{tt} + i\mu|\psi|^4\psi, \quad (1)$$

where  $z$  is the cavity round-trip number,  $t$  is the retarded time,  $\psi$  is the normalized envelope of the field,  $D$  is the group velocity dispersion coefficient with  $D = \pm 1$  depending on whether the group-velocity dispersion is anomalous or normal, respectively,  $\delta$  is the linear gain-loss coefficient,  $i\beta\psi_{tt}$  accounts for spectral filtering or linear parabolic gain ( $\beta > 0$ ),  $\epsilon|\psi|^2\psi$  represents the nonlinear gain (which arises, e.g., from saturable absorption), the term with  $\mu$  represents, if negative, the saturation of the nonlinear gain, the term with  $\nu$  corresponds, also if negative, to the saturation of the nonlinear refractive index.

We have to note that the variety of localized pulsating solutions found here results from the properties of the cubic-quintic CGLE. The higher-order nonlinear terms are important for the system to have pulsating solutions as well as period-doubling bifurcations. We have not observed these phenomena in the cubic CGLE. A system has to have a certain minimum complexity in its nonlinear properties in order to have *localized robust* pulsating solutions. The nonlinear terms in the case of the cubic CGLE are much simpler and,

as a result, the cubic CGLE in the (1+1) D case does not have such solutions. We recall, in this respect, that even stationary solitons of the cubic CGLE, in general, are not stable [34], and, quintic terms are essential for stable solitons to appear [22].

### III. NUMERICAL SCHEME

We have solved Eq. (1) using a split-step Fourier method for different initial conditions and for a great variety of values of the equation parameters in the anomalous dispersion regime, i.e., for  $D = +1$ . In general, we fix all the parameters except one of them (in most of the cases  $\epsilon$ , which stands for cubic gain when positive) and study the behavior of the solution as this parameter changes. We then change slightly another parameter ( $\nu$  generally) and repeat the above process.

The numerical simulations have been carried out using a split-step technique, with various step sizes down to 0.0001 along the  $z$  direction, with up to 16384 points along the  $t$  direction, to ensure that the results contain no numerical artifacts. The results were also checked using independent codes on various computers. The pulsating or chaotic nature of the solutions is an inherent property of these solitons for a given range of parameters, and is not a consequence of the discretization. We should also stress that the effect is not related to the homoclinic instabilities occurring in integrable [35] or Hamiltonian systems, as our equation is dissipative.

A big variety of localized solutions can be observed. Among them there are stable stationary pulses (solitons) [36], pulses of more complicated shape (composite solitons) [37], and moving solitons [34]. The topic of the research in this paper is the pulses that are globally stable as localized structures but continuously change their shape. The variety of these solutions can be even larger than that of stationary solitons. In this paper we concentrate mainly on breatherlike or pulsating solutions. In terms of the experiment this means that the laser pulse changes its amplitude, width, and energy in each successive round trip and this process is periodic in time. Periodicity does not necessarily have to be commensurate to the round-trip time. It is defined by the macroscopic physical parameters of the system and the only requirement is that it has to be larger than the round-trip time in order for the effects we have found to be observable.

### IV. PULSATING SOLITONS

In our previous work [36–38] we concentrated on stationary soliton solutions of the CGLE and in the regions of parameters where they exist. However, these are not the only possible type of solitons. Pulsating solitons are another example of localized structures. These are solutions whose profile evolves in  $z$ . They arise naturally from stationary ones when the latter become unstable. So far, we discovered several new types of cubic-quintic CGLE “robust” pulsating soliton solutions with complicated behavior. They exist in isolated regions of the parameter space, a fact that facilitates their identification as different solutions. All these solutions have two common features—they repeat periodically in the  $z$

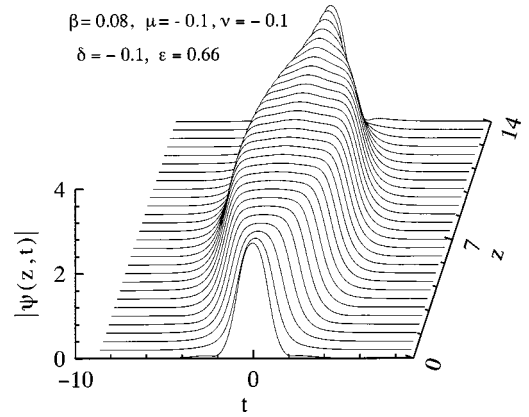


FIG. 1. Plain pulsating soliton of the CGLE. The parameters are  $D = +1$ ,  $\epsilon = 0.66$ ,  $\delta = -0.1$ ,  $\beta = 0.08$ ,  $\mu = -0.1$ , and  $\nu = -0.1$ . Only one period is shown.

direction (the propagation direction) and they are actually pulsating. We should say that there can be a great variety of pulsating structures.

The solutions we are presenting here have distinctive features, and this allows us to classify them as “plain pulsating,” “erupting,” or “exploding” solitons and “creeping” solitons. We have studied their main characteristics and investigated in detail the region in the parameter space where they exist. None of them can be found in analytic form, as it happens for the vast majority of the *stable* stationary solitons of the cubic-quintic CGLE [34]. Besides, pulsating solutions are generic in the sense that they occupy appreciable regions of the five-dimensional parameter space. In addition, they can be excited from a wide range of initial conditions. Eventually, and usually very quickly, each of them will converge to that pulsating soliton that exists for the given set of the equation parameters. An exception to this rule occurs when two or more solutions exist for the same set of parameters. When broad (but still localized) initial conditions are used, several pulsating solitons can be excited simultaneously.

#### A. Purely periodic pulsating soliton

An example of a pulsating soliton found numerically is shown in Fig. 1. It shows perfectly periodic behavior with the period in  $z$  being around 14. It has a different shape at each  $z$ , since it evolves, but it recovers its exact initial shape after a period. In this sense, we can call this type a “plain” pulsating soliton. Pulsating solutions have been found earlier by Deissler and Brand [26]. However, our new solutions do not belong to the class found in Ref. [26]. First, the dispersion parameter  $D$  in Ref. [26] has the opposite sign, so that the region of parameters where they exist is different. When changing  $D$  continuously, pulsating solitons cease to exist at  $D = 0$  so that there is not a continuous transformation of one into the other. Secondly, the profile of the periodic solutions in Ref. [26] changes only in the soliton tails whereas our pulsating soliton changes its shape quite appreciably. As a result, the value of energy in Ref. [26] stays almost constant, while in the case of the solution shown in Fig. 1, the energy,  $Q = \int_{-\infty}^{\infty} |\psi|^2 dt$ , changes from about 10 to 45. When we



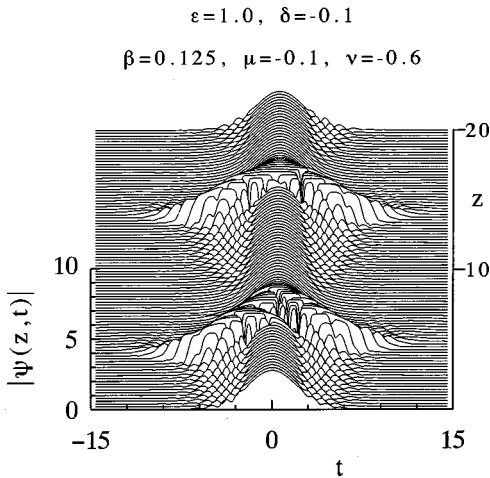


FIG. 2. Two periods of the evolution of an exploding soliton. The parameters are  $\epsilon=1.0$ ,  $\delta=-0.1$ ,  $\beta=0.125$ ,  $\mu=-0.1$ , and  $\nu=-0.6$ .

change the parameters of the equation, the solution remains pulsating in a finite region. As we mentioned above this region does not extend to the region with negative  $D$ .

### B. Exploding solitons

Another class of pulsating solitons can be called “exploding” or “erupting” [40] solitons. “Exploding” soliton evolution (see Fig. 2) starts from a stationary localized solution that has a perfect soliton shape. After a while, its “slopes” become covered with small ripples (a form of a small scale instability) that seem to move downwards along the two slopes of the soliton, and very soon the pulse is covered with this seemingly chaotic structure. When the ripples increase in size, the soliton cracks into pieces, like a mountain after a strong volcanic eruption or after an earthquake. This can also look like an explosion. This completely chaotic, but well-localized, structure then is filled with “lava,” which restores the perfect soliton shape after a “cooling” process. The process repeats forever, although the distance between “explosions” fluctuates, and in each of them the pulse splits into different pieces.

Needless to say, these solutions cannot be found in analytic form. However, they are as common as stationary solutions and exist for a wide range of parameters. The process never repeats itself exactly in successive “periods.” However, it always returns to the same shape. In this sense, the orbit that corresponds to this solution in each period is homoclinic.

Figure 3 shows the spectral width  $\sigma_F = \sqrt{\langle f^2 \rangle - \langle f \rangle^2}$ , where  $f$  is the frequency, versus the temporal width  $\sigma_T = \sqrt{\langle t^2 \rangle - \langle t \rangle^2}$  of the “exploding” soliton during several successive “periods” of explosion. Here,  $\langle t^n \rangle$  stands for  $\int_{-\infty}^{\infty} t^n |\psi|^2 dt / Q$ , and the same applies for  $f$  in the spectral domain. Although each part of the total trajectory starts and ends at the same point, which corresponds to the solution in the quiet part of the evolution, where it changes only slightly, they are all different during the “exploding” stage of the evolution. This shows that the evolution never repeats

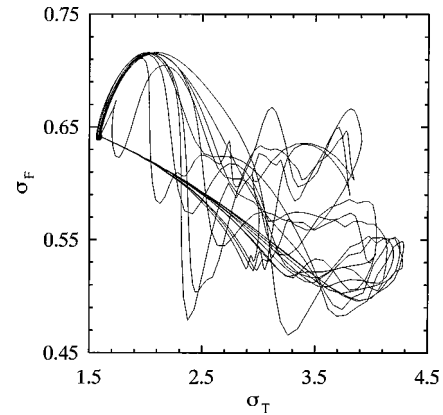


FIG. 3. The spectral width versus the temporal width for an erupting solitons during ten successive cycles. The parameters are the same as in Fig. 2.

itself and that each explosion is unique. Hence, the quiet stage of the soliton is an attractor, but is an unstable one. The length of each “period” also varies slightly, as it should for an attractor. The position of the pulse shifts slightly in  $t$  after each explosion and consequently the average position roams.

As seen from Figure 3, the product  $\sigma_F \sigma_T$  is around 1. This is in more than 10 times greater than the same product for bandwidth-limited pulses, which is  $1/4\pi \approx 0.08$ . This shows that the soliton is highly chirped and literally “tries” to split apart during the quiet regime of evolution. It is remarkable that the spectrum of the solitons becomes narrower during the burst (from  $\sigma_F \approx 0.64$  down to  $\sigma_F \approx 0.51$ ). However, the product  $\sigma_F \sigma_T$  increases during the explosion due to the chaotic structure of the solution in time. This product returns to its previous value when a new soliton emerges from the fragments of the burst. The growth rate of instability is actually complex and is equal to  $0.8 + 16.7i$  for this particular case. The imaginary part of the growth rate eigenvalue is responsible for the radiative structure around the soliton. The total energy in the soliton,  $Q$ , also pulsates and increases during the burst by almost a factor of 5 from its value in the quiet regime ( $Q=22$ ) up to  $Q=100$ .

Clearly, the exploding soliton is an example of a chaotic solution. The solution might enter this regime directly from purely periodic pulsating solutions when we change the parameters of the system. On the other hand, there are also chaotic solutions that always have a smooth transverse profile but it never repeats in evolution. This latter case can be reached from the pulsating solutions through period-doubling bifurcations. However, this happens in other areas of the system parameters.

### C. Creeping soliton

One more example of the class of pulsating solutions is the “creeping” soliton, which is shown in Fig. 4. It is a rectangular pulse with two fronts and a sink (due to energy loss) at the top. The two fronts pulsate back and forth relative to the sink asymmetrically at the two sides. As a result of this asymmetry, the position of the center-of-mass of the whole soliton shifts after each pulsation. The accumulated shifts result in the soliton motion with a constant velocity.

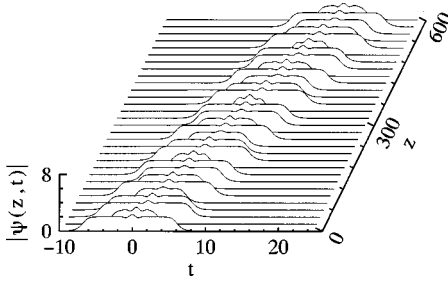


FIG. 4. Creeping soliton of the quintic CGLE. The parameters are  $D=+1$ ,  $\epsilon=1.3$ ,  $\delta=-0.1$ ,  $\beta=0.101$ ,  $\mu=-0.3$ , and  $\nu=-0.101$ .

This pulse coexists with the zero velocity soliton with two fronts, which are symmetrically pulsating at both sides. The shape of the creeping soliton resembles the shape of the composite soliton [34]. All pulsating solutions exist at the boundaries between solitons and fronts [41]. However, the region for “creeping” solitons is isolated from the region of “exploding” solitons. Therefore, each can be classified as a separate type of pulsating soliton.

We are confident that there might be more types of pulsating structures of the cubic-quintic CGLE. Their classification might comprise a topic of a special research. Pulsating solutions might have several frequencies in their motion and these solutions are quasiperiodic. A relatively simple case would be when the system has two frequencies. An explicit example is a moving pulsating solution, which instead of having a constant velocity moves forth and back around a fixed point. This solution is illustrated in Fig. 5. Obviously, there are two frequencies involved in this motion which, in general, are incommensurate. The more frequencies are involved into evolution, the more complicated is the dynamics. However, at this stage, we cannot predict how many frequencies would be involved in any particular case. Rather we can simulate solutions numerically and change the parameters continuously to see what kind of changes we can have.

Below, we concentrate on transitions between various types of pulsating solitons as well as on transition to local-

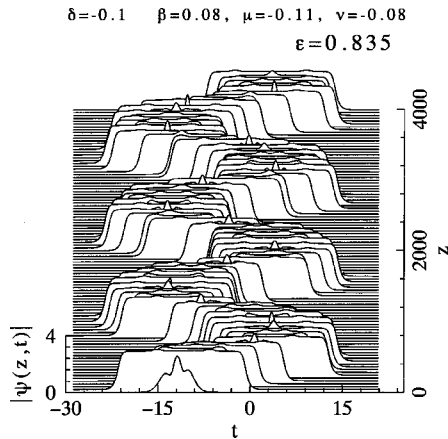


FIG. 5. Evolution of a moving periodic pulsating (creeping) pulses. The parameters in this case are  $D=+1$ ,  $\delta=-0.1$ ,  $\beta=0.08$ ,  $\mu=-0.11$ ,  $\nu=-0.08$ , and  $\epsilon=0.835$ .

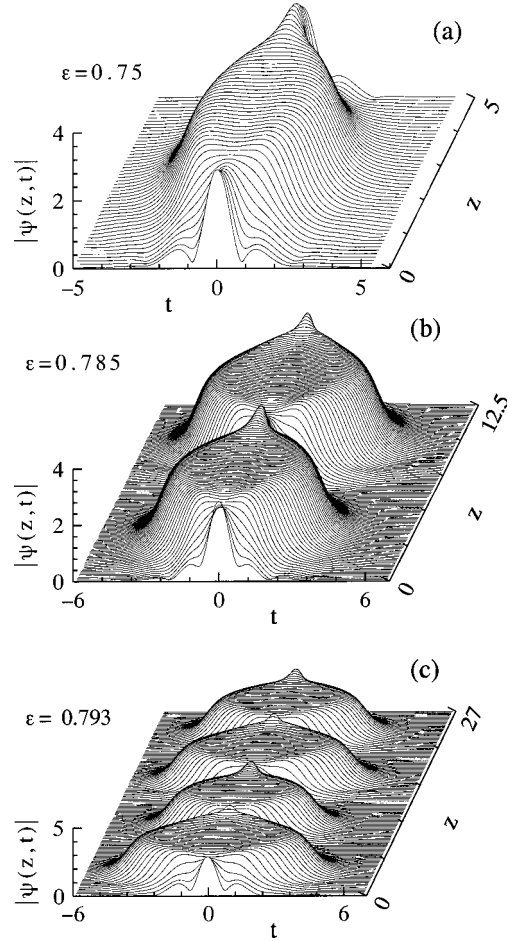


FIG. 6. Pulsating solitons of the CGLE. The two lower plots show (b) period doubling and (c) period quadrupling of pulsations in a  $z$  direction when parameter  $\epsilon$  changes. The parameters are  $D=+1$ ,  $\delta=-0.1$ ,  $\beta=0.08$ ,  $\mu=-0.1$ , and  $\nu=-0.07$ , and (a)  $\epsilon=0.75$ , (b)  $\epsilon=0.785$ , and (c)  $\epsilon=0.793$ .

ized structures that pulsate chaotically. The spectrum of the longitudinal evolution for the chaotic motion is, clearly continuous rather than discrete. There might be various scenarios of transition from discrete spectrum to a continuous one and one of them is the sequence of period-doubling bifurcations.

### V. PERIOD DOUBLING

A pulsating solution, which can bifurcate to double periodic pulsation, is shown in Fig. 6(a). The solution is strictly periodic when the pulse shape is repeated in each period of pulsation. We say it has double periodicity when the shape repeats itself after two pulsations. The transition from the former to the latter happens as period-doubling bifurcation when one of the parameters of the equation is changed. Figure 6(b) illustrates this process. Period quadrupling is observed when parameter  $\epsilon$  is increased as shown in Fig. 6(c). This route to chaos has the usual Feigenbaum type convergence with the differences in bifurcation points  $\epsilon_{n+1}-\epsilon_n$  converging geometrically [14] so that transition to chaos happens at finite  $\epsilon_\infty$ .

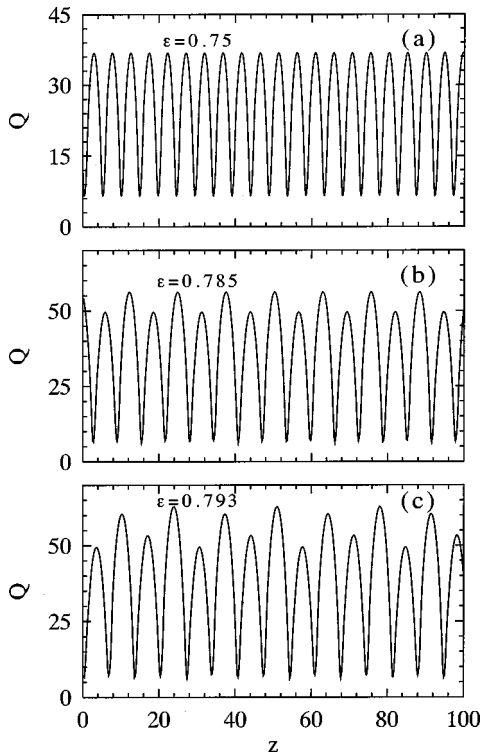


FIG. 7. Energy  $Q$ , versus  $z$  for the solutions whose pulse profiles are shown in Fig. 6. The two lower plots show clearly (b) period doubling and (c) period quadrupling.

Above the threshold value of  $\epsilon$  the pulse shape does not repeat itself in each pulsation and the behavior is chaotic. We stress that we are dealing with a single pulse but the shape of this pulse can change in an unpredictable way. This is different from the chaotic solutions to the CGLE in a transverse field profile when several pulses or other solutions can exist simultaneously and interact chaotically [42].

To illustrate the pulsating behavior of the pulses in more detail we calculated the pulse energy, which also changes in  $z$  along with the pulse shape. Figure 7 shows the energy  $Q$ , of the pulse versus  $z$  for the same solutions as in Fig. 6. As we can see, the pulse energy oscillates for period-1 pulsating solutions with a large amplitude, which shows that this is not a weak effect. The oscillations become more complicated when period doubling (b) and period quadrupling (c) phenomena take place. The maxima in the  $Q$  versus  $z$  plot then alternate such that every second or every fourth maximum repeat. After the transition to chaos through the sequence of period-doubling bifurcations occurs, all maxima in the  $Q(z)$  appear to be different from each other although the pulsating feature of the localized solution is clearly there.

To show the existence of bifurcations we constructed the Poincaré map of the periodic motion. In our case this map can be simplified and effectively made one dimensional. Therefore we shall plot a single parameter of the solution versus a single parameter of the equation. Namely, we use the following procedure. Starting with an arbitrary input, and for a given set of the values of the parameters, we propagate it a certain distance until any initial transient has died out and the solution is purely periodic or stationary. Then we moni-

tored each successive maximum in the  $Q$  versus  $z$  function for a certain  $z$  interval, typically set to 500. To minimize the initial transient the solution obtained for a certain  $\epsilon$  is taken as an initial condition for finding the corresponding solution for the next value of  $\epsilon$ . Usually we started with the lowest value of  $\epsilon$  in an interval of interest and monotonically increase it. When we observed an abrupt transition, we also moved backwards to see if any hysteretic behavior takes place.

In the following series of figures these maxima of  $Q(z)$  are given as functions of  $\epsilon$ , while the rest of the equation parameters are fixed. For strictly periodic pulsating solutions this technique gives a single point in the plot for each value of  $\epsilon$ . Bifurcation into double periodic pulsating solution gives two points in the plot. Period quadrupling bifurcation produces four points and so on. Chaotic solution generates a continuous vertical line. Sometimes two points indicate the existence of two different solutions instead of double period solutions. This case will be made clearly distinguishable in each figure.

To make sure that our simple technique adequately describes the phenomenon, we constructed also a two dimensional Poincaré maps. Namely, we do also monitor some other solution characteristics such as the peak amplitude or the pulse width. These plots are not shown here but using the more complicated technique we observed the same features of periodic or chaotic solutions as that deduced from monitoring  $Q$  only. In this way we were able to check that we were not missing some periodic or chaotic solutions that could nevertheless keep constant energy.

The plot in Fig. 8(a) is obtained using the above technique. It shows the peak value of  $Q$  for each oscillation of the pulsating solutions versus the parameter  $\epsilon$ . Note that stationary solitons can also be plotted in this figure. These solutions do not oscillate and the value of  $Q$ , which is constant, is simultaneously the peak value of  $Q$ . The curve denoted soliton pulses (SP) corresponds to such stationary pulses. The curve above it corresponds to the pulsating solutions. The fact that it is a single curve shows that pulsations are strictly periodic and have a unique period of oscillations. The first branching point at approximately  $\epsilon=0.786$  corresponds to period-doubling bifurcation. The second branching point at approximately  $\epsilon=0.8$  corresponds to period quadrupling bifurcations. The part of the plot in a dotted rectangle is zoomed in and shown separately in Fig. 8(b). It shows higher-order bifurcations and the full set of period doubling route to chaos. Note that we must use a finite step size in  $\epsilon$  (typically  $\Delta\epsilon=0.0002$ ), which does not have enough resolution to show the actual threshold where the transition to chaos happens. Nevertheless, this is exactly Feigenbaum-type route to chaos, which has all the features of this well-known phenomenon.

Above the threshold, chaotic solutions exist for a certain interval of values of  $\epsilon$ , once the rest of the parameters is fixed. Varying  $\epsilon$ , we fix the direction towards the region of chaos, which occupies a certain region in the parameter space. We could also change any other parameter instead of  $\epsilon$  and keep the rest fixed or we could change simultaneously several parameters moving along a certain direction in the

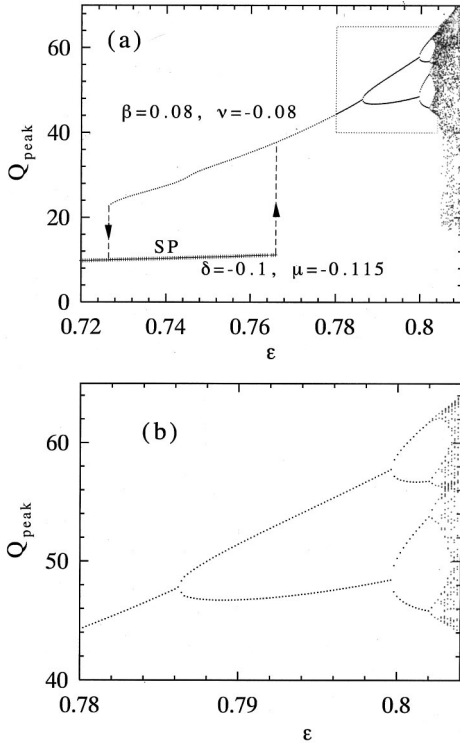


FIG. 8. One-dimensional Poincaré map: (a) Peak energy versus  $\epsilon$  for pulsating and stationary solitons. The arrows in (a) show the directions in which the transition from pulsating to stationary pulses takes place when  $\epsilon$  changes. The right-hand side of the curve for pulsating solutions in (a) shows the sequence of period-doubling soliton bifurcations and burst into chaos. (b) Magnified part of the plot, which is framed by dots in (a). The values of the parameters are  $\beta=0.08$ ,  $\nu=-0.08$ ,  $\delta=-0.1$ , and  $\mu=-0.115$ .

parameter space. These directions are not all equivalent and the route to chaos can vary. Some examples are shown below.

Finally we should add that although it happens very rarely we have also seen period-2 moving solitons.

## VI. COEXISTENCE OF PULSATING, CHAOTIC, AND STATIONARY SOLITONS

It is remarkable and surprising that pulsating solutions are fixed in the same way as stationary pulses. Namely, the solution  $\psi(z,t)$  is a unique function of  $z$  and  $t$  at each set of equation parameters. This makes solitons in dissipative systems different from those in integrable ones where solitons are one- or two parameter families. Besides, in nonintegrable but Hamiltonian systems, pulsating solitons do not exist. Even, if pulsations exist at the beginning due to specially chosen initial conditions, they die out during propagation [24]. In the CGLE case, pulsating solitons do exist and if periodic, they are fixed. Once the set of parameters is given, any initial condition always converges to the same pulsating solution unless two of them exist simultaneously for the same set of parameters, being both stable. It can also happen that several (more than two) fixed but qualitatively different solutions exist and are stable for the same set of parameters.

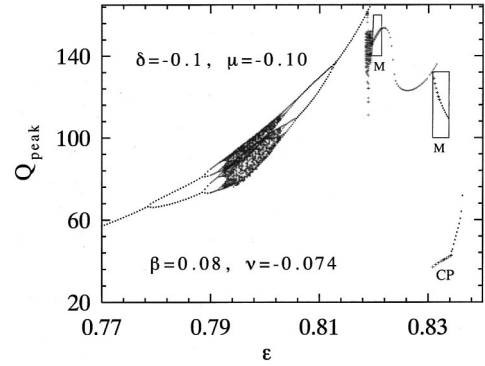


FIG. 9. One-dimensional Poincaré map: (a) Two sequences of period-doubling soliton bifurcations. Bifurcations occur when the parameter  $\epsilon$  approaches the region of chaos at  $0.792 < \epsilon < 0.803$  from the left as well as from the right. Solutions in the two small rectangles correspond to moving pulsating solitons. The pulsating solutions located in the right-hand side (larger) rectangle coexist with the stable composite solitons and with period-1 pulsating solitons. The branch for the composite solitons is denoted CP. The simulation parameters are  $D=+1$ ,  $\delta=-0.1$ ,  $\beta=0.08$ ,  $\mu=-0.1$ , and  $\nu=-0.074$ .

Figure 8(a) shows, in particular, that the branch of pulsating solutions exists simultaneously with stationary pulses in the interval of  $\epsilon$  from  $\approx 0.726$  to  $\approx 0.766$ . The branch for the latter is denoted SP. This would not be surprising as we know already that various stationary solitons can coexist [34]. Moreover, up to five different “stable” solutions may exist simultaneously [39]. However, stationary solutions are solutions of an ordinary differential equation (ODE), which realize a minima of an operator in a functional space, and to switch from one minimum to another, an appreciable perturbation is needed. In the case of pulsating solutions, we cannot reduce the problem to an ODE and the notion “minimum of an operator” cannot be applied directly. It might be a “valley” in the functional space and it has to be separated from the minimum corresponding to a stationary solution. Only when the parameters of the system change so much that one of the solutions ceases to exist, can it be transformed into another type. This process is shown in Fig. 8(a) by the arrows. Namely, in this figure we have the hysteretic cycle between the stationary plain pulse solutions and the single periodic solutions. In this case these two kinds of solutions coexist for a large interval of values of  $\epsilon$ . As we will show in the next section, this region of coexistence depends very much on the value of the other parameters.

Figure 9 shows an example of chaotic behavior, which is located in the region of  $0.792 < \epsilon < 0.803$ . When changing  $\epsilon$  provided that other parameters are fixed, the transition to chaos occurs from the left as well as from the right. Each of these routes to chaos are through the sequence of period-doubling bifurcations. A second small region of chaotic behavior of pulsating solitons appears at  $\epsilon \approx 0.819$ . It appears without period-doubling bifurcations although solitons are strictly periodic at the left-hand side from this region as well as at the right-hand side.

The solutions shown inside the small rectangles M are moving pulsating solitons and they are similar to the solu-



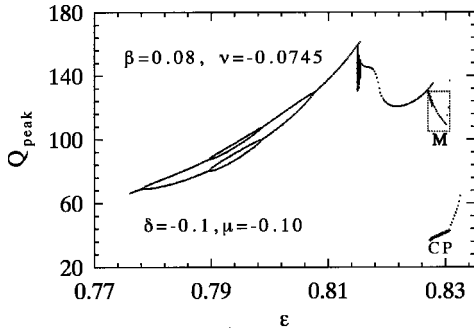


FIG. 10. One-dimensional Poincaré map: example of period doubling soliton bifurcations when  $\nu$  is slightly shifted relative to the case presented in the previous figure. The region of chaos in this case disappears. Moving pulsating solitons in the box M coexist with the composite pulses (CP) and period-1 pulsating solitons (above the box M). The simulation parameters are:  $D = +1$ ,  $\delta = -0.1$ ,  $\beta = 0.08$ ,  $\mu = -0.10$ , and  $\nu = -0.0745$ .

tions shown in Fig. 4. The moving solitons in the right-hand side rectangle at  $\epsilon > \approx 0.83$  coexist with zero velocity pulsating solitons whose energy  $Q$  is above the rectangle. Simultaneously these two pulsating solutions co-exist with stationary composite pulses (the latter are described in the book [34]). This example shows the possibility of co-existence of three different solitons for the same values of the equation parameters; two of them are pulsating and one is a stationary soliton.

If we slightly change the parameter  $\nu$  to the value 0.0745 (see Fig. 10), the region of chaos disappears. The whole sequence of period-doubling bifurcations also disappears and only period 2 and period 4 solutions can be observed. Correspondingly, we have only two period-doubling bifurcations on the way to the right and two period-doubling bifurcations on the way to the left. This example shows that period-doubling bifurcations do not necessarily lead to chaos unless some other parameters of the system are properly changed in order to reach the region of chaos. As in Fig. 9, the moving pulsating solutions are enclosed in a rectangle labeled M. Only one of these regions is left at this value of  $\nu$ . The tristability situation still remains.

When the parameter  $\nu$  is shifted further down to 0.066 (Fig. 11), the region of chaotic behavior reappears. It appears as a sequence of period-doubling bifurcations from the left, at  $\epsilon \approx 0.796$ . However, an interesting feature of this region is that in the middle of the region of chaotic solutions, period-5 and period-6 solutions emerge. Their region of existence vary with  $\nu$  but remarkably enough, there is not any period jumping bifurcations at the boundaries of their existence. Or at least they cannot be seen with the resolution in  $\epsilon$ , which we are using ( $\Delta\epsilon < 0.0002$ ). Period-4 solutions appear also in a small interval around  $\epsilon \approx 0.833$  without being preceded by period-2 solutions.

Figure 11 gives also an example of the coexistence of pulsating solutions with chaotic pulsations. Namely, black triangles represent a pulsating period-2 solution, which is different from the solutions in the region of chaos. Which one appears depends on the initial conditions. However, once excited, each of these solutions evolves without transforma-

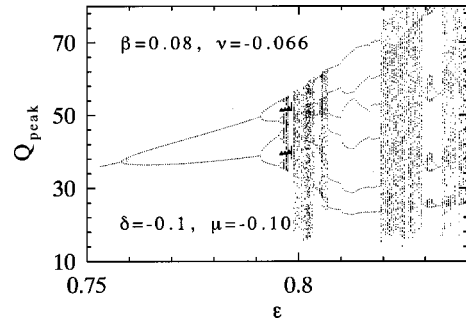


FIG. 11. One-dimensional Poincaré map: one more example of period-doubling soliton bifurcations. Transition to chaos occurs only from the left. The region of chaotic behavior is located at  $0.798 < \epsilon < 0.826$ . It is interrupted by the period-5 solutions (at  $\epsilon \approx 0.804$ ) and period-6 solutions (at  $0.807 < \epsilon < 0.819$ ). Black triangles correspond to a period-2 solutions, which are different from the chaotic solitons. The parameters in this case are  $D = +1$ ,  $\delta = -0.1$ ,  $\beta = 0.08$ ,  $\mu = -0.10$ , and  $\nu = -0.066$ .

tion into another one unless we reached the edge of the region for the existence of some particular solution. This shows, first, that pulsating solutions are globally stable, or, better to say, robust. Second, chaotic pulsations in this example are completely separated in a functional space from the regular pulsating solutions resulting in their coexistence. Third, the solid triangles in Fig. 11 are visibly located at the continuation of period-2 curves at the left. Clearly, period-2 solutions lose their stability after the period quadrupling bifurcation but recover their stability again at higher  $\epsilon$ .

We can find some indirect confirmation for the existence of unstable period-2 solutions in the region of chaos in Fig. 12. Here, the parameter  $\nu$  is further decreased to  $-0.064$  and the other parameters are not changed. We can see clearly the appearance of period-2 solutions at  $\epsilon \approx 0.792$  with the chaotic pulsations being suppressed. As in the previous case, the curves for the period-2 solution appear to be a visible continuation of the two curves at the left before period quadrupling bifurcation happens. We can guess that the period 2 solutions do exist all the way between the intervals where it

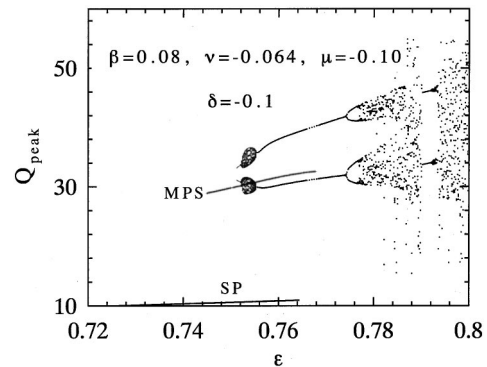


FIG. 12. One-dimensional Poincaré map: an example of period-2 chaotic solitons (two black spots). Multiple bifurcations do not happen. Moving pulsating solutions coexist with plain pulsating solutions, with chaotic solutions and with stationary pulses (SP). The values of the parameters in this case are  $D = +1$ ,  $\delta = -0.1$ ,  $\beta = 0.08$ ,  $\mu = -0.10$ , and  $\nu = -0.064$ .



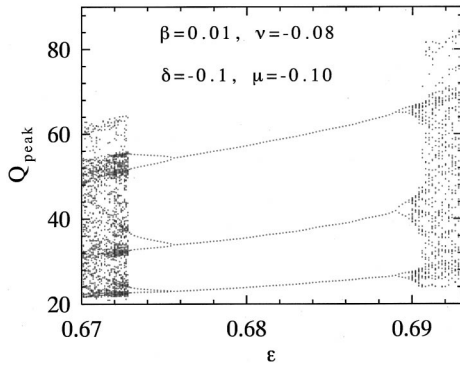


FIG. 13. One-dimensional Poincaré map: peak energy versus  $\epsilon$  for pulsating and stationary solitons. Period-3 and period-6 solutions are surrounded by chaotic behavior. The parameters in this case are  $D = +1$ ,  $\delta = -0.1$ ,  $\beta = 0.01$ ,  $\mu = -0.1$ , and  $\nu = -0.08$ .

is stable but lose its stability and become “invisible.”

Moreover, we can also guess that the chaotic pulsations in Fig. 11 are the consequence of several periods of oscillations that are incommensurate and can be considered as internal modes of the system. At some values of the parameter  $\epsilon$ , certain modes suppress all others and as a result we have period-5 and period-6 solutions. In Fig. 12, the period-2 mode suppresses the others in a small interval of  $\epsilon$ .

Another interesting feature of the plot in Fig. 12 is the period-2 chaos at  $\epsilon \approx 0.753$ . This is a chaotic solution with two frequencies, i.e., taking every second maximum in the  $Q$  versus  $z$  plot, we obtain a perfectly periodic sequence. However, two consecutive maxima show chaotic features, which is the reason for the appearance of the two black “balls” in the middle of the period-2 branches. Transition to chaos occurs at the two sides of this chaotic region abruptly without the sequence of period-doubling bifurcations.

It is remarkable that this period-2 chaos coexists with moving pulsating solitons (denoted MPS) and with stationary soliton pulses denoted SP. The range of existence of the two latter solitons is wider than the period-2 chaos and they are shown by the corresponding lines in the plot. As we can see, the tristable behavior of solutions is more the rule rather than exception. The new fact here is that chaotic solutions coexist with plain stationary solitons and with moving pulsating solitons (like “creeping” structure showed in Fig. 4).

Period quadrupling bifurcation in Fig. 12 occurs at  $\epsilon = 0.774$  and the direct transition to chaos without any further sequence of period-doubling bifurcations at  $\epsilon = 0.779$ . Definitely, the sequence of period-doubling bifurcations is not the only route that can lead to chaos, but many other scenarios are possible.

Figure 13 shows an example of the period-3 solutions. The horizontal lines on the plot correspond to the three successive energy maxima of soliton pulsations. The region of their existence extends from  $\epsilon \approx 0.676$  until  $\epsilon \approx 0.689$ . At the edges of this interval, the solution bifurcates and transforms into period-6 solutions. Both intervals of period-6 solutions are much shorter than the interval for period-3 solutions. At the outer edges with  $\epsilon \approx 0.673$  and  $\epsilon \approx 0.69$ , period-6 solutions in turn bifurcate into chaotic pulsations with the  $Q_{\text{peak}}$  covering continuously a finite interval along the vertical axis.

There is not any other period jumping bifurcations between the period-6 solutions and chaotic pulsations. In this respect, we have to mention that period-3 and period-6 bifurcations have been observed in the nonlinear fiber ring resonator [10]. Although no direct comparison with the experiment is possible, qualitatively this phenomenon finds a natural explanation in the CGLE model.

Our numerical examples show that there is a multiplicity of scenarios of transition to chaotic behavior. Which particular scenario appears, depends completely on the direction we choose to move in the five-dimensional space. It follows from this analysis that the best way would be to find the boundaries in the five-dimensional parameter space between the regions with qualitatively different solutions and move in the directions normal to those boundaries. This is a complicated and highly computer-time consuming task but can be carried out to some extent if we find at least the projections of these regions on two-dimensional planes of the parameter space. We have done this work here for several such planes.

## VII. REGIONS OF EXISTENCE OF PULSATING SOLITONS IN THE PARAMETER SPACE

The regions of pulsating solitons and the regions of chaotic pulsations are regions in a five-dimensional parameter space, i.e., in the space of  $\beta$ ,  $\mu$ ,  $\nu$ ,  $\epsilon$ , and  $\delta$ . In order to have solutions in the form of localized structures we have to restrict the values of this parameter. Namely,  $\epsilon > 0$ ,  $\delta < 0$ ,  $\mu < 0$ ,  $\beta > 0$ , and  $\nu < 0$ . The condition  $\delta < 0$  is required to keep the zero background to be stable. The condition  $\epsilon > 0$  ensures that there is a positive gain in the system. The condition  $\mu < 0$  allows to saturate the nonlinear gain in order to keep the soliton amplitude being limited from above and  $\nu < 0$  saturates the nonlinear Kerr effect. Finally, the condition  $\beta > 0$  provides transverse stability to the soliton. The above restrictions allow us to limit the boundaries for search of pulsating localized structures. The dispersion  $D$  can have either sign for the CGLE to have localized pulsating solutions. We have chosen  $D$  to be positive as, to our knowledge, no one observed pulsating solitons in this case before. The actual value of  $D$  can be rescaled to one without loss of generality.

With the above restrictions we are still faced to deal with a five-dimensional space of parameters, although now it is only one “quadrant” of this space. Obviously, we can only present two-dimensional slices of these regions. Nevertheless, these slices give enough information to see interrelations between various types of solitons. We shall present those regions along with the ones for stable stationary solitons, which at certain conditions might overimpose. Our paper also shows that the transition to chaos is a complicated phenomenon and depends very much on which border is crossed during the transition.

To illustrate the fact that the route to chaos depends on the way of crossing the boundary of the region of chaos, we started our calculations with the two-dimensional regions on the  $(\epsilon, \nu)$  plane. These regions are shown in Fig. 14. There are five main areas on this plot. The lowest region (vertically hatched area) corresponds to plain stationary pulses (stable stationary solitons). Stationary solitons were the main object

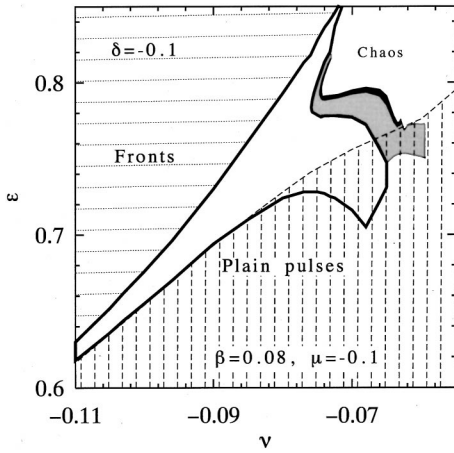


FIG. 14. The region of existence of stationary pulses (vertically hatched area), pulsating solitons (enclosed in a thick line), period doubled (gray area) fronts (horizontally hatched area) and chaotic solutions on the plane  $(\nu, \epsilon)$ . The narrow dark region between chaotic solutions and period-doubled pulsating solitons corresponds to period-4 solutions. The parameters of the simulation are  $D = +1, \delta = -0.1, \beta = 0.08$ , and  $\mu = -0.1$ .

of study in our previous work [36]. We should mention here that our technique only gives stable structures although unstable solitons can also exist in these areas. Unstable solitons cannot appear explicitly but they can play a certain role in the general dynamics.

Above this vertically hatched region the soliton solutions are pulsating. This means that stationary pulses become unstable in this region and longitudinal modulation instability transforms them into plain pulsating solitons. The pulsations have a single period of oscillation. The region for pulsating solitons is enclosed within a thick solid line.

The region up and to the left of pulsating solutions (horizontally hatched area) corresponds to fronts. The width of solitons in each pulsation [similar to the one in Fig. 6(a)] becomes so wide that the two fronts at each side of the soliton are not bounded anymore and move away from each other. It is remarkable that for this set of parameters there is not a simple transition between the solitons and fronts as predicted in Ref. [41]. The boundary between the region of stationary solitons and fronts is a stripe, which corresponds to pulsating solitons. In this region, the two interacting fronts are not bounded strongly enough to comprise a stationary structure but the bounding energy is enough for them to oscillate relative to each other.

The upper-right (white) region on this plane corresponds to chaotic pulsations. Below this region, solutions go through the sequence of period-doubling bifurcations. In particular, period-2 solutions exist in the gray area and period-4 solutions in the black stripe. Further period-doubling areas cannot be resolved in the scale of this plot. However, it is clearly seen that pulsating solitons can enter the region of chaos without the sequence of period-doubling bifurcations at the boundary above the shaded regions. In a five-dimensional parameter space the routes to chaos can take various forms.

The Fig. 14 also shows that stationary pulses can coexist with plain pulsating solitons and with period-2 pulsating so-

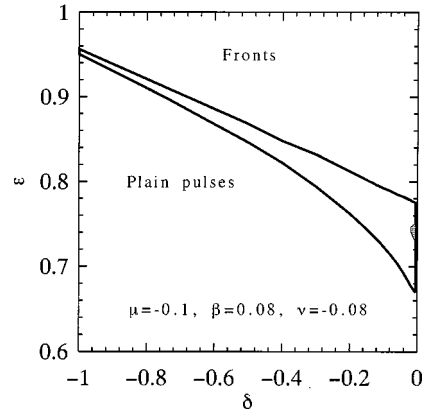


FIG. 15. The region of existence of stationary plain pulses, pulsating solitons (central triangular stripe) and fronts on the plane  $(\delta, \epsilon)$ . The small shaded region inside the region of pulsating solutions corresponds to period-2 solutions. The parameters of simulation are  $D = +1, \beta = 0.08, \mu = -0.1$ , and  $\nu = -0.08$ .

lutions. Clearly, there is not a direct smooth transition from one to another in these regions. They are separated in energy by some gap, which means that they are located far enough in the functional space from each other, being independent solutions.

Another slice of the five-dimensional space of parameters is shown in Fig. 15. This is the  $(\delta, \epsilon)$  plane. It shows again that the stripe of pulsating solutions divides this plane into regions of stationary solitons and fronts. The region of period-doubled pulsating solutions in this case is located inside the region for periodic pulsations. They exist only in a hardly appreciable region for very low values of  $|\delta|$ .

One more slice of the region of existence of pulsating solutions is shown in Fig. 16. This is the  $(\beta, \epsilon)$  plane. Topologically this slice is similar to the one presented in Fig. 14. The area of stationary solitons occupies most of this plot. It is vertically hatched. Fronts exist in the upper part inside the area hatched horizontally. The stripe of pulsating solutions

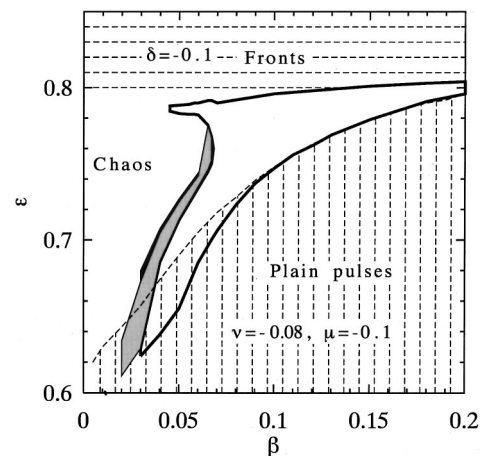


FIG. 16. The region of existence of plain pulses, pulsating solitons (central triangular area), and chaotic solitons on the plane  $(\beta, \epsilon)$ . The values of the rest of the parameters are  $D = +1, \delta = -0.1, \mu = -0.1$ , and  $\nu = -0.08$ .

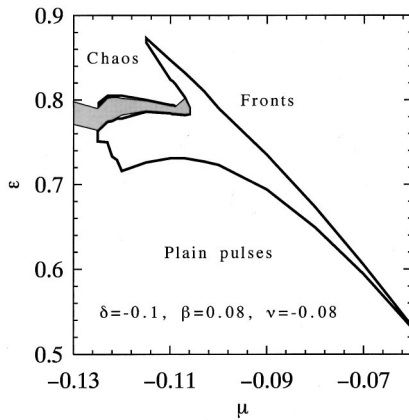


FIG. 17. The region of existence of plain pulses, pulsating solitons (central triangular stripe), fronts and chaotic solitons on the plane  $(\mu, \epsilon)$ . The parameters of the simulation are  $D=+1$ ,  $\delta=-0.1$ ,  $\nu=-0.08$ , and  $\beta=0.08$ .

separates the regions for stationary solitons and fronts. Regular pulsating solitons become chaotically pulsating in the left-hand side white area. Transition to chaos happens both through the sequence of period-doubling bifurcations and directly at the boundary defined by the thick solid line. The region of period-2 solutions is shown as a gray area and the region of period-4 solutions as a black area. Period-8 solutions and higher are located between the period-4 and chaos regions but it is unresolvable in the scale of this plot. We can say definitely that the region for the stationary solitons has a common area with the regions of pulsating solitons with single and double periods as it is shown in Fig. 16. However, it is difficult to draw a border between the fronts and chaotically pulsating solutions. This can be a topic of a separate investigation.

Figure 17 shows the region of existence of these solutions in the plane  $(\mu, \epsilon)$ . The topological structure of this slice is similar to the previous Fig. 16. Stationary solitons are located at low  $\epsilon$  and low negative  $\mu$ . Stationary solitons become unstable at the upper boundary of their existence and transform into pulsating solitons in the triangular region in the middle of the plot. Above the triangle only fronts exist. The upper-left corner of the plot corresponds to chaotic pulsations. Transition from the single frequency pulsations to chaotic pulsations happens through the sequence of period-doubling bifurcations as well as directly at the lower boundary of the “beak” on the top of the triangular region.

Exploding solitons shown in Fig. 2 represent a special type of chaotic localized structures, which are qualitatively different from the chaotic pulsations with continuous spectrum. We would expect that their region of existence would be very small. However, this is not true. Figure 18 shows the region of existence of exploding solitons in the  $\nu$ - $\epsilon$  plane. The area where these solutions exist is surprisingly wide. Say, in the middle of the plot, the parameter  $\epsilon$  can be changed three times and these solutions still exist. Parameter  $\nu$  changes twice from the right-hand side of the plot to the left-hand side. Figuratively speaking, these solutions cannot be “missed.” In the lower limit in  $\epsilon$ , these solutions either become periodic solutions or are extinguished completely. In

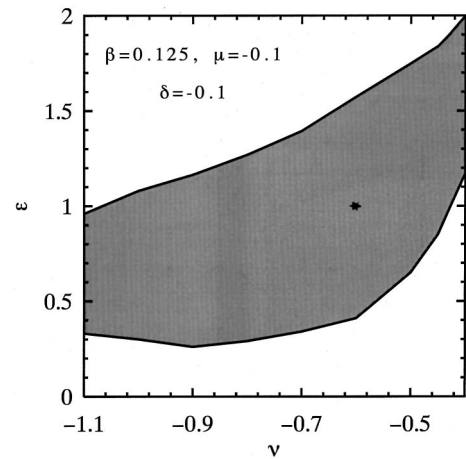


FIG. 18. Region in the parameter plane  $(\nu, \epsilon)$  where exploding solitons exist. The star shows the point where the simulations for Fig. 2 were done. Other parameters are  $\delta=-0.1$ ,  $\beta=0.125$ , and  $\mu=-0.1$ .

the upper limit, above the shaded strip, they become either chaotic or stationary pulses.

## VIII. DISCUSSION

The slices we presented here are to some extent chosen by chance. The regions of pulsating solutions occupy an appreciable part of the five-dimensional parameter space. We tried to choose the regions that contain the samples presented in Sec. IV. At the same time we tried to cover the most interesting parts of this five-dimensional space. We can say with a certain degree of confidence that there is nothing special happening if we extend the range of parameters beyond those we have chosen in Figs. 14–17. Nevertheless, this area is still open for investigations and deserves more efforts. By far, we can say confidently the following:

(1) We have found new pulsating solutions of the cubic-quintic CGLE. This fact shows that dissipative systems can have strictly periodic localized structures in contrast to Hamiltonian systems, which don’t have such solutions. Pulsating solutions of the CGLE cannot be obtained as perturbations of breathers of the nonlinear Schrödinger equation.

(2) There are several types of pulsating solutions, which roughly can be classified into plain pulsating (with single period of pulsations), quasiperiodic (with several periods involved in the pulse dynamics), exploding soliton, which can be considered as a special type of attractor, creeping solitons, which are pulsating moving localized structures, and chaotic pulsating solitons, which have a continuous spectrum of pulsations.

(3) Each of the above solutions exists in certain regions of parameters in the five-dimensional space. The regions of existence of pulsating localized structures are comparable or even larger than regions for stationary solitons. Each pulsating soliton exists in an isolated region so that we can classify each of them as a different type of soliton. Crossing the borders of these regions results in the transformation of the solution into another type (into stationary soliton, front or chaotic soliton).



(4) In some regions of parameters, solutions of various types can coexist resulting in a bistable and tristable behaviors. In particular, we have found the regions of coexistence for plain stationary or composite stationary solitons with moving pulsating and plain pulsating solitons. There are also the areas of coexistence between chaotic pulsating solitons and plain pulsating solitons. Double periodic solitons can coexist with both chaotic solitons and plain stationary solitons. This list can be continued.

(5) The transition between regular pulsations and chaotic pulsations can happen as a single bifurcation as well as a sequence of bifurcations including the sequence of period-doubling bifurcations. More exotic structures like “double periodic chaotic soliton” can also appear.

(6) The regions of chaotic solitons contain soliton solutions, which are not stable but play a certain role in the overall dynamics. We have found examples of double-periodic solutions being located inside the regions of chaotic solutions. They might become unstable but continue to exist in wide range of parameters. It is very likely that this coexistence of unstable solitons with stable pulsating ones gives rise to the chaotic localized structures. However, the latter assertion needs more investigations to draw definite conclusions.

Our results are quite general and cannot be directly applied to any particular experiment. However, the knowledge we extracted from this study can be used to analyze the experimental data. Passively mode-locked lasers with fast saturable absorbers have all the physical effects, which are described by the CGLE. Namely, the generation of short pulses

is defined by the balance between the dispersion and nonlinearity as well as the balance between the gain and loss. The real system has also spectral filtering components. This means that qualitatively these effects can be observed in real systems, and after rectification, can find certain applications.

## IX. CONCLUSIONS

In conclusion, we have found, new fascinating types of pulsating solitons predicted by the quintic complex Ginzburg-Landau equation. Namely, different types of localized pulsating solutions such as plain pulsating, exploding, creeping, and chaotic solutions have been found. Period- $N$  solutions, where  $N$  takes almost any integer value, have been also predicted. The route to chaos by period-doubling bifurcations has been exhaustively studied, and although being quite common is not the only way to chaos we present in this paper. The regions of existence of various types of solutions have been calculated in the five-dimensional parameter space. The latter revealed large areas where various types of pulses coexist resulting in the effects of bistability and tristability.

## ACKNOWLEDGMENTS

The work of J.M.S.C. was supported by the Dirección General de Enseñanza Superior under Contract Nos. PB96-0819 and BFM2000-0806, and by the Australian Research Council. N.A. and G.T. are members of the Australian Photonics Co-operative Research Centre (APCRC).

- 
- [1] L.F. Mollenauer and R.H. Stolen, *Opt. Lett.* **9**, 13 (1984).
  - [2] H.A. Haus and M.N. Islam, *IEEE J. Quantum Electron.* **QE-21**, 1172 (1985).
  - [3] S.M.J. Kelly, *Opt. Commun.* **70**, 495 (1989).
  - [4] F.X. Kärtner, I.D. Jung, and U. Keller, *IEEE J. Sel. Top. Quantum Electron.* **2**, 540 (1996).
  - [5] G. Carpintero and H. Lamela, *J. Appl. Phys.* **82**, 2766 (1997).
  - [6] D. Coté and H.M. van Driel, *Opt. Lett.* **23**, 715 (1998).
  - [7] G. Sucha, S.R. Bolton, S. Weiss, and D.S. Chemla, *Opt. Lett.* **20**, 1795 (1995).
  - [8] G. Sucha, D.S. Chemla, and S.R. Bolton, *J. Opt. Soc. Am. B* **15**, 2847 (1998).
  - [9] Liguó Luo, T.J. Tee, and P.L. Chu, *J. Opt. Soc. Am. B* **15**, 972 (1998).
  - [10] S. Coen, M. Haelterman, Ph. Emplit, L. Delage, L.M. Simohamed, and F. Reynaud, *J. Opt. Soc. Am. B* **15**, 2283 (1998).
  - [11] M. Haelterman, *Appl. Phys. Lett.* **61**, 2756 (1992).
  - [12] J. Boyce and R.Y. Chiao, *Phys. Rev. A* **59**, 3953 (1999).
  - [13] V.N. Chizhevsky and R. Corbalán, *Phys. Rev. E* **53**, 1830 (1996).
  - [14] M.J. Feigenbaum, *J. Stat. Phys.* **19**, 25 (1978).
  - [15] Y.H. Kao and H.T. Lin, *Phys. Rev. A* **48**, 2292 (1993).
  - [16] A.N. Pisarchik and R. Corbalán, *Phys. Rev. E* **59**, 1669 (1999).
  - [17] B. Thédrez, J.G. Provost, and R. Frey, *Opt. Lett.* **14**, 958 (1989).
  - [18] N. Piovella, P. Chaix, G. Shvets, and D.A. Jaroszynski, *Phys. Rev. E* **52**, 5470 (1995).
  - [19] S. Colin, E. Contesse, P. Le Boudec, G. Stephan, and F. Sanchez, *Opt. Lett.* **21**, 1987 (1996).
  - [20] H. Haus, *J. Appl. Phys.* **46**, 3049 (1975).
  - [21] P.A. Belanger, *J. Opt. Soc. Am. B* **8**, 2077 (1991).
  - [22] J.D. Moores, *Opt. Commun.* **96**, 65 (1993).
  - [23] A.I. Chernykh and S.K. Turitsyn, *Opt. Lett.* **20**, 398 (1995).
  - [24] D. Artigas, L. Torner, and N. N. Akhmediev, *Opt. Commun.* **143**, 322 (1997).
  - [25] J. Satsuma and N. Yajima, *Prog. Theor. Phys. Suppl.* **55**, 284 (1974).
  - [26] R.J. Deissler and H.R. Brand, *Phys. Rev. Lett.* **72**, 478 (1994).
  - [27] P.-S. Jian, W.E. Torruellas, M. Haelterman, S. Trillo, U. Peschel, and F. Lederer, *Opt. Lett.* **24**, 400 (1999).
  - [28] C.O. Weiss, *Phys. Rep.* **219**, 311 (1992).
  - [29] A.M. Dunlop, E.M. Wright, and W.J. Firth, *Opt. Commun.* **147**, 393 (1998).
  - [30] V.B. Taranenko, K. Staliunas, and C.O. Weiss, *Phys. Rev. A* **56**, 1582 (1997).
  - [31] W.J. Firth and A.J. Scroggie, *Phys. Rev. Lett.* **76**, 1623 (1996).
  - [32] N. N. Rozanov, *Optical Bistability and Hysteresis in Distributed Nonlinear Systems* (Physical and Mathematical Literature Publishing Company, Moscow, 1997).
  - [33] P.K. Jakobsen, J.V. Moloney, A.C. Newell, and R. Indik, *Phys. Rev. A* **45**, 8129 (1992).

- [34] N. N. Akhmediev and A. Ankiewicz, *Solitons: Nonlinear Pulses and Beams* (Chapman and Hall, London, 1997).
- [35] M. J. Ablowitz and P. A. Clarkson, *Solitons, Nonlinear Evolution Equations and Inverse Scattering*, London Mathematical Society Lecture Notes Series Vol. 149 (Cambridge University Press, Cambridge, 1991).
- [36] J.M. Soto-Crespo, N.N. Akhmediev, and V.V. Afanasjev, *J. Opt. Soc. Am. B* **13**, 1439 (1996).
- [37] V.V. Afanasjev, N.N. Akhmediev, and J.M. Soto-Crespo, *Phys. Rev. E* **53**, 1931 (1996).
- [38] N.N. Akhmediev, V.V. Afanasjev, and J.M. Soto-Crespo, *Phys. Rev. E* **53**, 1190 (1996).
- [39] N. N. Akhmediev and J. M. Soto-Crespo, in *Proceedings of SPIE* (International Society for Optical Engineering, Bellingham, WA, 1999), Vol. 3666, pp. 307–316.
- [40] J. M. Soto-Crespo, N. N. Akhmediev, and A. Ankiewicz, *Phys. Rev. Lett.* (to be published).
- [41] V. Hakim, P. Jakobsen, and Y. Pomeau, *Europhys. Lett.* **11**, 19 (1990).
- [42] A. Torcini, H. Frauenkron, and P. Grassberger, *Phys. Rev. E* **55**, 5073 (1997).